Soils and Foundations 2012;52(2):207–215

The Japanese Geotechnical Society

Soils and Foundations

www.sciencedirect.com
journal homepage: www.elsevier.com/locate/sandf

Combined effects of strain rate and temperature on consolidation behavior of clayey soils

Ayato Tsutsumi[a,*], Hiroyuki Tanaka[b]

[a]Foundations Group, Geotechnical Engineering Field, Independent Administrative Institution, Port and Airport Research Institute, Japan
[b]Division of Field Engineering for the Environment, Graduate School of Engineering, Hokkaido University, Japan

Available online 11 April 2012

Abstract

It is considered that the long term settlement of clay deposits, known as secondary consolidation, is caused by clay viscosity. In this paper, the viscous property of clayey soils is examined from two viewpoints: one is temperature and the other is the effect of the strain rate. To investigate these effects, a special constant rate of strain (CRS) loading test, in which the strain rate is changed during the test, was carried out at temperatures of 10 and 50 °C on reconstituted clay samples. Under the normal strain rate, such as the order of $10^{-6}\,s^{-1}$, well-known temperature effects on the consolidation behavior were confirmed. That is, the high temperature condition leads to increased hydraulic conductivity due to the reduction in the viscosity of pore water at higher temperatures. It is also observed that the yield consolidation stress decreases with increasing temperature due to the viscous properties of soil skeletons. However, it is found that with higher temperature and smaller strain rates, the clay specimen does not follow conventional viscous behavior, like the Isotache model, but the gradient of stress–strain curve considerably decreases. The reason for different behavior from the Isotache model may be attributed to the creation of a new structure to resist the external deformation, under high temperature and a slow strain rate.

Keywords: Clay; One-dimensional consolidation; Strain rate effect; Temperature effect

1. Introduction

The long term settlement of soft clay deposits after the dissipation of excess pore water pressure, which is sometimes called secondary consolidation or creep deformation, has been an important but difficult issue in geotechnical engineering. A consensus seems to exist among researchers that such creep settlement is caused by viscous properties of the clay skeleton. Hence, it is very important to understand and evaluate the viscous behavior of clayey soils in order to predict the ground settlement during and after dissipation of the excess pore water pressure with more accuracy. In the laboratory, the viscosity can be expressed in terms of the strain rate effect in one-dimensional consolidation tests, and test results may be interpreted by consolidation models which take the strain rate into consideration. A typical model is the Isotache model proposed by Šuklje (1957). In the Isotache model, the compression behavior is determined by the order of the strain rate (see for example, Leroueil et al., 1985; Imai and Tang, 1992; Imai et al., 2003; Tanaka, 2005a and b; Watabe et al., 2008). Kobayashi et al. (2005) have reported that the Isotache model provides accurate predictions of the settlement in the Pleistocene clay layers at the Kansai International Airport, Japan, than the conventional Terzaghi's consolidation model. However, making settlement based on the Isotache model requires the consolidation soil parameters under extremely

*Corresponding author.
E-mail address: tsutsumi-a@pari.go.jp (A. Tsutsumi).

Peer review under the responsibility of The Japanese Geotechnical Society
http://dx.doi.org/10.1016/j.sandf.2012.02.001

Production and hosting by Elsevier

small strain rates in the field, i.e., smaller than $10^{-10}\,s^{-1}$ (see Leroueil, 2006).

Tsutsumi and Tanaka (2011) have developed a special CRS test apparatus and conducted the CRS test, in which the strain rate is changed during the test from 10^{-6} to $10^{-10}\,s^{-1}$. According to the Isotache model, when the strain rate is changed, the stress–strain curve immediately shifts to that corresponding to the new strain rate, and as expected, when the strain rate suddenly decreased, the effective stress decreased due to the viscous property of clay skeleton. However, some interesting behavior was also observed: the clay specimen under very small strain rates did not follow the stress–strain curve expected from the Isotache model. Actually, gradient of the curve was markedly smaller than that of virgin compression curve, which the specimen would be expected to follow if the strain rate was not changed. Furthermore, when the strain rate went back to the original rate from very small strain rates, the stress–strain curve overshot the expected virgin compression curve, as if the clay specimen had developed structure in the previous loading process under small strain rates. Hence, the Isotache model cannot be directly applied to the compression behavior under small strain rates. Such non-Isotache stress–strain behaviors have also been reported by Tatsuoka et al. (2008), who conducted drained triaxial compression tests for granular materials. They proposed other viscosity models, such as TESRA, Combined and P & N.

It is well known from previous studies that the viscous property of soft clayey soils is strongly related not only to the strain rate, but also to temperature: the yield consolidation pressure decreases with increasing temperature (see for example, Eriksson, 1989; Boudali et al., 1994; Akagi and Komiya, 1995; Marques et al., 2004). In addition, another important temperature effect on consolidation has been reported: the development of a structure resisting deformation accelerates under long-term consolidation at high temperature (see Tsuchida et al., 1991; Towhata et al., 1993). Change in the temperature may provide a clue for understanding the non-Isotache behavior reported by Tsutsumi and Tanaka (2011). In this study, CRS consolidation tests with varying strain rates at different temperature levels were carried out for three different clayey soils.

2. Testing method and samples

2.1. CRS test apparatus and testing procedures

In order to study the temperature effect, it is preferable to carry out CRS test using the same specimen, i.e., by changing the temperature during the testing, to avoid any differences in soil properties for different specimens. However, changing the temperature during the testing is very difficult in practice. When the temperature is changed, the measuring system as well as the specimen itself is influenced. One example is the zero drift of the sensors. For this reason, the CRS tests were carried out at two constant temperatures: 50 and 10 °C. Although it is recommended to carry out the CRS test under large different temperature levels to identify the temperature effect, the sustainability of the test is very important to obtain stable test data for a long period of more than a week. Taking into account these demands and the capability of the apparatus used in this study, testing temperatures of 50 and 10 °C were adopted.

The CRS apparatus followed JIS A 1227 (Japanese Standards Association, 2009b): the specimen was 60 mm in diameter and 20 mm in initial height. Fig. 1 shows a schematic view of the consolidation cell. Drainage was allowed through the upper end of the specimen. The bottom of the specimen was connected to a transducer to measure the water pressure. The load generated by applying a constant strain was measured by a load cell at the bottom of the consolidation cell. A back pressure of 100 kPa was applied to assure good saturation of the specimen during the test. The effective vertical pressure (p') was calculated assuming that the excess pore water pressure in the specimen is distributed in a parabolic manner as expressed by the following equation:

$$p' = \sigma - \frac{2}{3}\Delta u \quad (1)$$

where σ is the total pressure on the specimen and Δu is the excess pore water pressure.

To generate a stable and extremely small strain rate, a special loading apparatus was developed, consisting of a Step Motor System whose resolution is as accurate as 2,621,440 pulses per revolution, and this was controlled by a personal computer (see Tsutsumi and Tanaka, 2011).

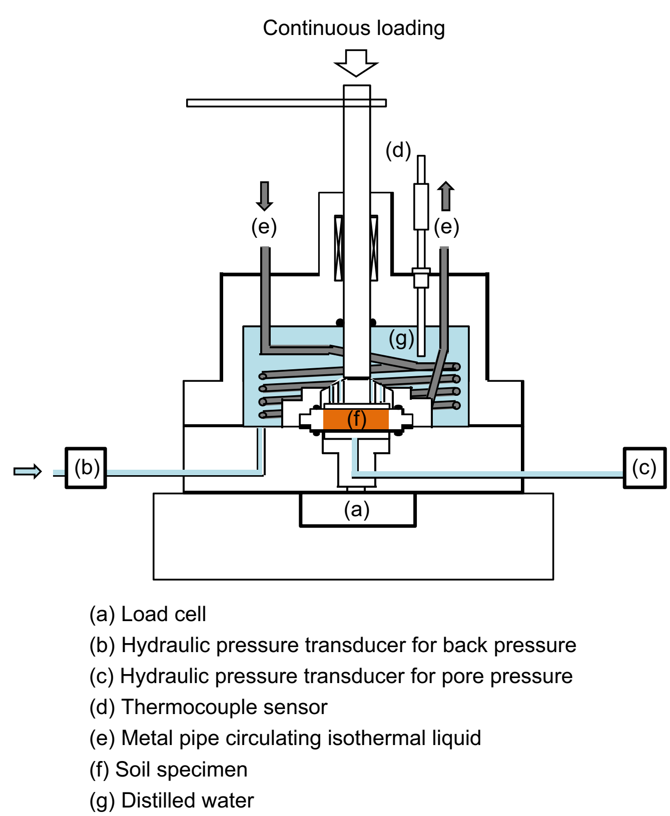

Fig. 1. Schematic view of consolidation cell.

The displacement was not measured by a conventional dial gauge, but obtained directly by counting the number of revolutions of the step motor and corrected by the deformation of the apparatus system, derived mainly from the deformation of the load cell. This correction was done based on a loading test without a soil specimen. The strain (ε^{T}) used in this paper is not the natural strain but the nominal strain, and the strain rate ($\dot{\varepsilon}^{T}$) is defined as the incremental nominal strain per increment in time.

As shown in Fig. 1, a metal pipe was spiraled around the specimen and an isothermal liquid was circulated through this pipe to control the temperature (T), which was measured by a thermocouple attached to the upper side of the consolidation cell. The preparation procedure for the testing was as follows: to avoid the offset drift of measuring instruments due to changes in the temperature, the whole CRS testing apparatus was preliminarily kept under a testing temperature by circulating isothermal liquid for at least 6 h, which were confirmed to be sufficient to reach a constant state when the temperature was increased from 25 to 50 °C. Then, records of P, u and u_b were initialized at the atmospheric pressure and a specimen was placed in a consolidation ring as quickly as possible. The consolidation ring with the specimen was mounted on the consolidation cell and fixed by the loading piston. The consolidation cell was filled with distilled water and a hydraulic pressure of 100 kPa was applied as the back pressure. The consolidation cell was heated or cooled again at the prescribed temperature for more than half a day, which was considered to be long enough for the specimen to be uniformly expanded or compressed.

2.2. Tested samples

Reconstituted samples were made at laboratory instead of using intact samples, to avoid the variability in soil properties for tested samples and to identify only the temperature effect. Three different clays were used in this study. A sample named as OsakaMa12 was collected from the construction site of the Kansai International Airport in the Osaka Bay, Japan. The second sample was obtained from the Louiseville site along the St. Lawrence River in Quebec, Canada. The third sample was a commercial powder clay named as Kasaoka. From the previous research (Tsutsumi et al., 2011), it was found that the stress–strain relationships of Osaka clay followed the isotache, while Louiseville clay strongly exhibited non-isotache behavior. Therefore, these two clays were selected to study the temperature as well as strain rate effects. Furthermore, Kasaoka clay, which is easily available, was also used. Their main geotechnical properties are shown in Table 1, where ρ_s, w_n, w_L, w_P and I_P are the density of soil particles, natural water content, liquid limit, plastic limit and plasticity index, respectively.

These clay samples and powder were consolidated in an acrylic cylinder under a consolidation pressure of 100 kPa after thoroughly remolding by a soil mixer at the water content about two times w_L. The value of w_n in the table is water content at trimming the specimen. As shown in the table, difference in w_n for each sample is so small that the influence of variability of the specimens can be ignored.

3. Test results

3.1. Evaluation of clay particles expanding due to change in temperature

Before discussing the temperature effect on consolidation properties, the influences of heating are examined on the change in the unit weight of the clay particles (ρ_s) and the pore water (ρ_w) in the soil specimen. The change in ρ_s ($\Delta\rho_s$) can be described by the following equation:

$$\Delta\rho_s = -\frac{\alpha_s \Delta T}{1+\alpha_s \Delta T}\rho_s \tag{2}$$

where α_s is the thermal coefficient of volume expansion of clay particles and ΔT is the change in temperature. Campanella and Mitchell (1968) have reported that α_s for usual soils varies from 1.5 to 5.2×10^{-5} per °C. Let us consider the change in void ratio (e) due to the change in temperature. Assumed conditions are as follows: temperature varies from 10 to 50 °C; α_s of 3.3×10^{-5} per °C; e and ρ_s are 2 and 2.7 at 10 °C, respectively. The change in ρ_w from 10 to 50 °C is 0.9997–0.9880, according to the Chronological Scientific Table (2004). Using these parameters, the change in e is calculated under these two conditions: freely deformed and completely confined. When the temperature changes 10–50 °C, e of 2.0 becomes 2.021 in the former case and 1.996 for the latter case. These differences are small enough to be ignored, considering an

Table 1
Geotechnical properties of studied clay samples.

Sample name	ρ_s (g/cm^3)	w_n (%)	w_L (%)	w_P (%)	I_P	T (°C)
Kasaoka	2.610	45.8	62	36	26	50
Kasaoka	2.610	45.5	62	36	26	10
OsakaMa12	2.657	81.9	109	43	66	50
OsakaMa12	2.657	82.0	109	43	66	10
Louiseville	2.767	47.6	71	22	49	50
Louiseville	2.767	47.7	71	22	49	10

experimental error. Therefore, it can be concluded that the volume expansion and the change in e due to the change in temperature is neglected in this study.

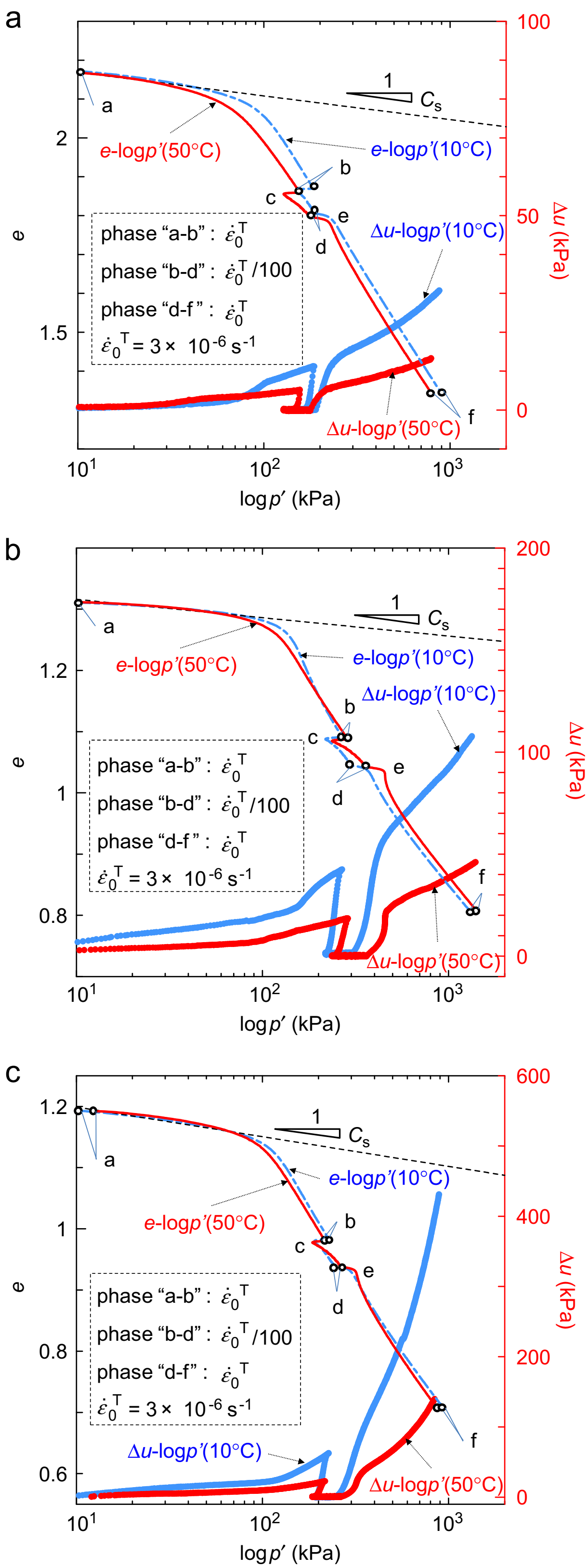

Fig. 2. The e-log p' and Δu-log p' relationships obtained from CRS tests for (a) OsakaMa12, (b) Louiseville and (c) Kasaoka.

3.2. Temperature effects on permeability

Fig. 2 shows the relationships between $\Delta u - \log p'$ and $e - \log p'$ obtained from the CRS tests for the three tested clays: (a) OsakaMa12, (b) Louiseville and (c) Kasaoka. The testing was performed at a constant T value of 10 or 50 °C, while the strain rate was changed during a test. The $e - \log p'$ curve segments between Points a and b as well as d and f were obtained under the reference strain rate of $3 \times 10^{-6}\ \mathrm{s}^{-1}$ ($\dot{\varepsilon}_0^T$) and that between Points b and d under $\dot{\varepsilon}_0^T/100$. Fig. 2(a) through (c) shows that Δu generated at 50 °C is clearly smaller than that at 10 °C. It is considered that such a difference in Δu is caused by different hydraulic conductivity (k). According to JIS A 1227 revised in 2009, k may be calculated as follows:

$$k = \frac{\rho_{\mathrm{wT}} g_{\mathrm{n}} \dot{\varepsilon} H_0 H_t}{2\Delta u} \tag{3}$$

where g_n, H_0 and H_t are the acceleration of gravity, specimen heights at initial and at each moment (t), respectively. In this equation, k is directly determined by CRS test, and its theoretical basis was reported in Geotechnical Testing Journal by Moriwaki and Umehara (2003). The relationships of e-log k are shown in Fig. 3(a) and (b), where the k values were indicated at only normally consolidated (NC) states and they were not calculated in the phase "b–d", because the strain rate was so small that the value of Δu was nearly zero and could not be measured with sufficient accuracy. When k at 50 and 10 °C is denoted, respectively, as k_{50} and k_{10}, k_{50} is larger than k_{10} and the e-log k relationships for k_{50} and k_{10} are parallel to each other, as shown in the figures. This means that the ratio of k_{50}/k_{10} is constant at the same e value.

It is well known that the viscosity of water is strongly influenced by temperature. Indeed, in the testing method of permeability defined by JIS A 1218 (Japanese Standards Association, 2009a): the measured k value is calculated at 15 °C (k_{15}), taking account of the change in the water viscosity due to temperature. The ratio of k_{50}/k_{10} is represented by Eq. (4) with the viscosity coefficient of pure water (η_T).

$$\frac{k_{50}}{k_{10}} = \frac{\eta_{10}}{\eta_{50}} \tag{4}$$

The ratio η_{10}/η_{50} is calculated to be 2.39 based on η_T of pure water given in the Chronological Scientific Table (2004). As shown in Fig. 3(a) and (b), the ratios of k_{50}/k_{10} for tested clays are in a relatively narrow range between 2.44 and 2.98, which is very close to the ratio η_{10}/η_{50}. Therefore, it may be concluded that the changes in k and Δu with T are caused by those of the water viscosity.

3.3. Temperature effects on compressibility under large strain rate

It was reported by Eriksson (1989) that as temperature becomes higher during incremental loading (IL) consolidation tests, stress–strain relationships shift leftward as shown in Fig. 4, i.e., the yield pressure decreases with an

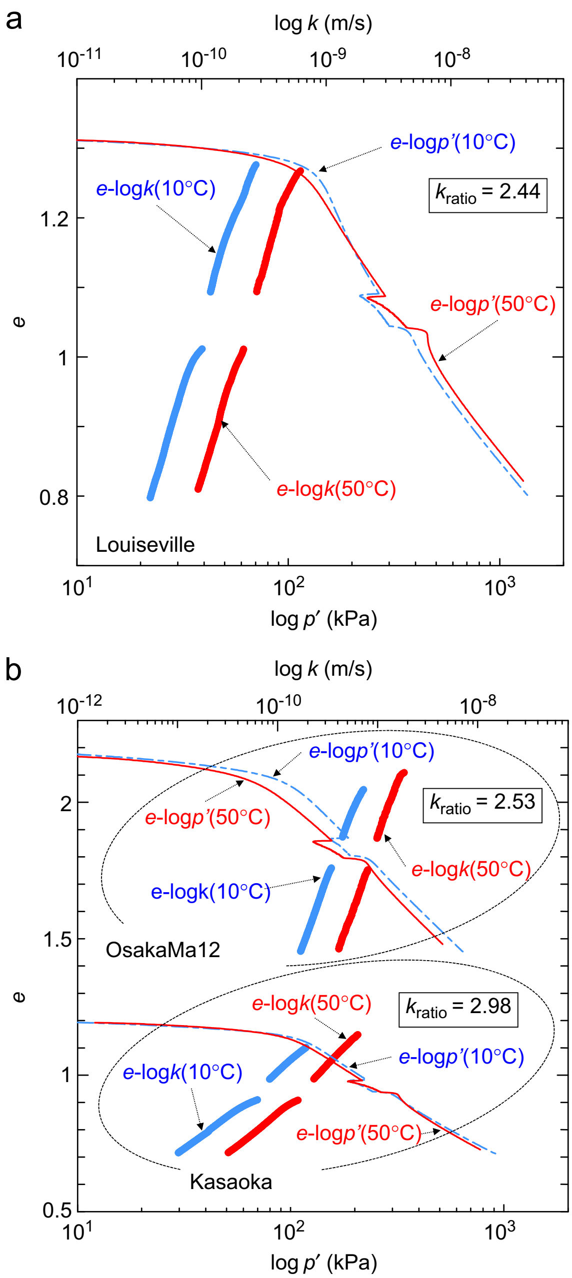

Fig. 3. The variation of hydraulic conductivity with void ratio for (a) Louiseville and (b) OsakaMa12 and Kasaoka.

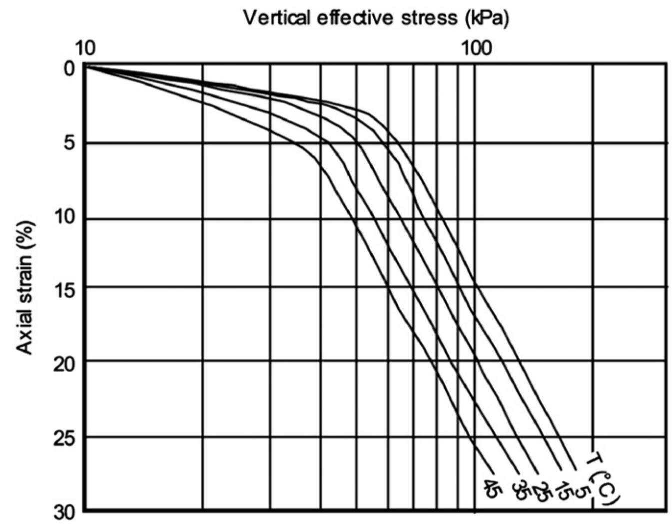

Fig. 4. Temperature effect on compression curves (after Eriksson, 1989).

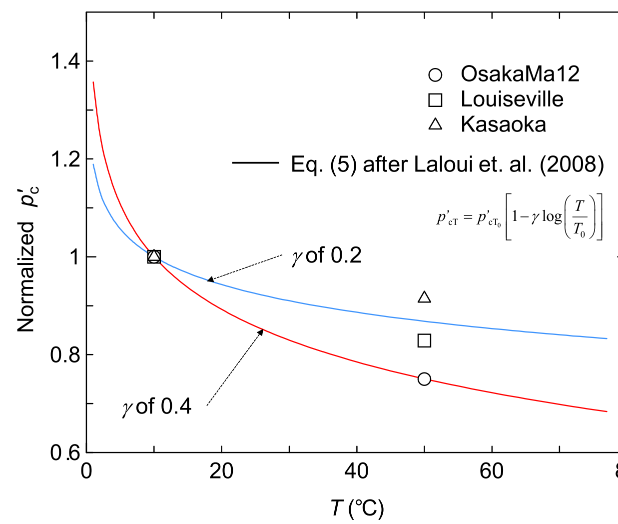

Fig. 5. Normalized p_c' value for studied clays and based on Eq. (5) against T.

increase in temperature. The temperature effect on compressibility under constant strain rates are examined by comparing the e-log p' curves at the temperatures of 10 and 50 °C, as shown in Fig. 2(a) through (c). It is observed the e-log p' curve at high temperature shifts to the left side. The amount of the shift can be expressed by the difference in the effective yield stress (p'_c). To observe the influence of T on p_c', the p_c' values for the studied clays are plotted against T in Fig. 5, where p_c' is normalized by the p_c' at 10 °C. It can be seen from the figure that p_c' decreases with an increase in T: i.e., all the studied clays exhibit viscous behavior due to high temperature. However, the degree of the influence of T is considerably different for the three clays.

The temperature effect on p_c' has been formulated in previous studies by, e.g., Moritz (1995), Marques et al. (2004) and Laloui et al. (2008). According to Laloui et al. (2008), for example, the p_c' value is represented as a function of T by the following equation:

$$p'_{cT} = p'_{cT_0}\left[1-\gamma\ \log\left(\frac{T}{T_0}\right)\right] \quad (5)$$

where p'_{cT} and p'_{cT_0} are the effective yield stresses at temperatures of T and T_0, respectively; γ is the material parameter peculiar to a given soil. Laloui et al. (2008) reported that γ can be related to w_L, and increases with w_L. In the present study, w_L ranges from 62% to 109%, corresponding to γ values of approximately 0.2 and 0.4, respectively, according to their study. Using these γ values, p_c'values calculated by Eq. (5) are also plotted in Fig. 5, normalized by p_c' at 10 °C. It can be seen from this figure that the normalized p_c' at 50 °C in this study follows well the tendency calculated by Eq. (5).

In addition to the decrease in the p'_c value due to high temperature, it can be recognized that the gradient of e-log p' relationship at the normally consolidated (NC) state, i.e., C_c under the high temperature is smaller than that at low temperature. The e-log p' curve for Louiseville clay at 50 °C crosses the curve at 10 °C because of the small C_c. This means that the p'_c values decrease with increasing temperature; however, such an effect disappeared with a decrease in e. This behavior is completely different from that presented in Fig. 4.

3.4. Temperature effects on compressibility under small strain rate

It is clearly observed in Fig. 2 that as the strain rate was changed, $e-\log p'$ curves shifted due to the strain rate effect, regardless of the temperature conditions. The strain rate effect is conventionally considered relevant only to the viscous component of sample deformation. For example, in the Isotache model, the total strain (ε^T) is assumed to consist of the elastic strain (ε^e) and the visco-plastic strain (ε^{vp}), as indicated in the following equation:

$$\varepsilon^{vp} = \varepsilon^T - \varepsilon^e \quad (6)$$

To examine the change of p' due to a change in strain rate at different temperature conditions in more detail, e-log p' relationships are rearranged as the relationship between ε^{vp} and p'. In this study, ε^T is the nominal strain not the natural strain, i.e., incremental total strain ($\Delta\varepsilon^T$) is defined as follows:

$$\Delta\varepsilon^T = \frac{\Delta e}{1+e_0} \quad (7)$$

where Δe and e_0 are incremental and initial e, respectively. Following conventional constitutive models, incremental ε^e ($\Delta\varepsilon^e$) is represented as follows:

$$\Delta\varepsilon^e = \frac{C_s}{1+e_0}\Delta \log p' \quad (8)$$

where C_s is the swelling index defined as the gradient of the e-log p' relationship at over consolidated (OC) states. To evaluate strain rate effects at various T, an important question arises as to whether C_s depends on T or not. Indeed, in previous studies, two opposite opinions have been reported. For example, Graham et al. (2001) reported the variation of C_s with T, while Yashima et al. (1998) adopted C_s independent of T in their model. As shown in Fig. 2, the e-log p' relationships before reaching p'_c, i.e., in the range of 10–70 kPa are almost independent of T. Therefore, it is assumed in this study that C_s is independent of T and $\Delta\varepsilon^e$ is calculated using the slope of e-log p' relationships before reaching p'_c as shown in Fig. 2, where the e-log p' relationships for 10 and 50 °C are nearly identical.

Fig. 6(a) through (c) shows magnified relationships between ε^{vp} and p', where the p' is normalized by the effective stress (p'_1) at the point of "b", just before the

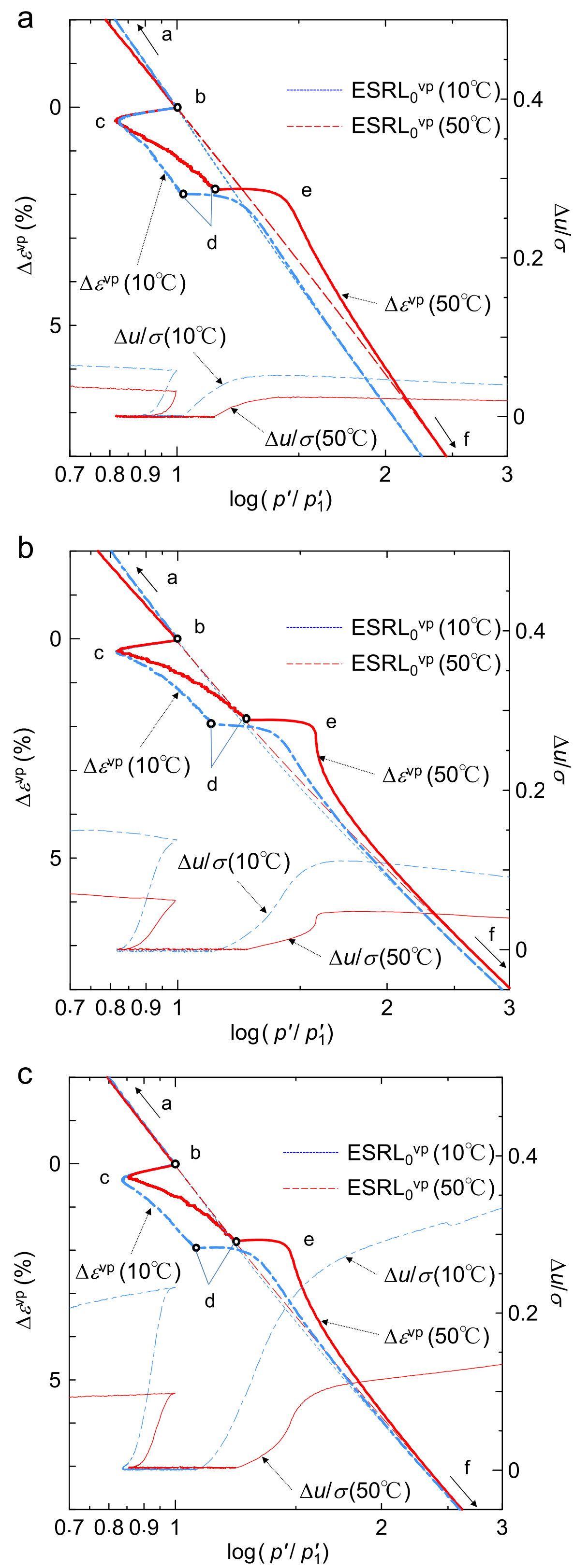

Fig. 6. The relationships between incremental visco-plastic strain, excess pore water pressure ratio and normalized effective stress for (a) OsakaMa12, (b) Louiseville and (c) Kasaoka.

strain rate is decreased, and the vertical axis indicates the incremental ε^{vp} from ε^{vp} at p'_1 ($\Delta\varepsilon^{vp}$). In these figures, Points a through f correspond to those in Fig. 2(a) through (c), and visco-plastic strain rate ($\dot{\varepsilon}^{vp}$) is defined as the incremental visco-plastic strain per unit time. Here, the reference equi-strain rate line ($ESRL_0^{vp}$) is defined as an $\varepsilon^{vp} - \log p'$ relationship that a specimen may follow if $\dot{\varepsilon}^{vp}$ is not changed. Tsutsumi and Tanaka (2011) assumed that the $ESRL_0^{vp}$ can be expressed by a cubic function and the constants in the equation were obtained by the least square fitting. The $ESRL_0^{vp}$ relationships for 10 and 50 °C were calculated by this method and presented by broken lines. The relationship between the excess pore water pressure ratio ($\Delta u/\sigma$) and p'/p'_1 is also shown in this figure.

The first interesting finding from Fig. 6(a) and (b) is that for both temperatures, p' decreases with a decrease in the strain rate due to the viscous property of soils, and this decrease in terms of the ratio p'/p'_1 is not significantly influenced by T. All clays exhibited almost the same minimum p'/p'_1 ratios caused by decreasing $\dot{\varepsilon}^{vp}$, regardless of temperature levels.

After p'/p'_1 attained the minimum value, the compression behavior seen in Fig. 6 was strongly influenced by temperature. At the phase of "c–d", where the strain rate becomes constant at $\dot{\varepsilon}_0^{vp}/100$, the $\Delta\varepsilon^{vp} - \log(p'/p'_1)$ curve at 50 °C for all the tested clays approached the $ESRL_0^{vp}$. At the phase of "d–e–f", where the strain rate returned to the original rate of $\dot{\varepsilon}^{vp}_0$, the curve considerably overshot the $ESRL_0^{vp}$. On the other hand, the $\Delta\varepsilon^{vp} - \log(p'/p'_1)$ curve at the phase of "c–d" at 10 °C is almost parallel with the $ESRL_0^{vp}$ and the amount of the overshoot on returning the original strain rate is considerably smaller than that at 50 °C. It can be considered that the specimen at high temperature and very small strain rate has gained the ability to resist the external deformation, as if the specimen has developed new structure. A similar phenomenon is observed even in the $e - \log p'$ relationship under the reference strain rate of $10^{-6}\,s^{-1}$. That is, as already mentioned, C_c at 50 °C is smaller than that at 10 °C, although this difference is not significant. This tendency is more prominent under the condition of the extremely small constant strain rate of $\dot{\varepsilon}_0^{vp}/100$.

4. Discussions

Two important effects caused by the changing temperature were identified in this study. One is the so-called viscous behavior due to high temperature conditions observed in the phase of "a–b" in Fig. 2: that is, p'_c decreases with an increase in T. Another effect is the gaining of the ability to resist deformation, i.e., decreasing C_c with an increase in T. This effect becomes much more prominent when the strain rate is smaller, as observed in the phase of "c–d" under $\dot{\varepsilon}_0^{vp}/100$ in Fig. 6; normalized p' at given $\Delta\varepsilon^{vp}$ is larger for higher T. As a result, in the phase of "d–e–f" in Fig. 6, the $\Delta\varepsilon^{vp} - \log(p'/p'_1)$ curve at 50 °C considerably overshoots the corresponding $ESRL_0^{vp}$, as if the clay specimen experienced aging in the previous phase of "c–d". However, this overshoot is destructed by the

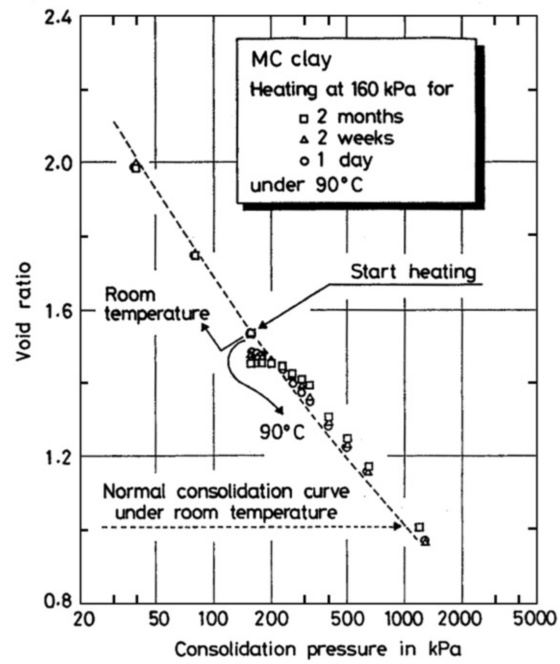

Fig. 7. Thermal aging behavior due to high temperature after Towhata et al. (1993).

faster loading under $\dot{\varepsilon}^{vp}_0$ and the $\Delta\varepsilon^{vp} - \log(p'/p'_1)$ curves return to their original trend.

According to Tsuchida et al. (1991), heating provides the same effect as aging on clay samples. They mentioned that this aging is caused by cementation and this cementation is accelerated by heating. A similar aging effect was also reported by other researchers, e.g., Towhata et al. (1993) and Akagi (1994). In Fig. 7, cited from Towhata et al. (1993), clay samples were subjected by incremental step loadings after applying a load of 160 kPa at 90 °C for various durations of time. The $e - \log p'$ relationship for heated samples shifts to higher p' in comparison to the reference relationship obtained by the end of primary consolidation indicated by the dotted line. They considered that such an aging effect was caused by the acceleration of secondary consolidation: i.e., clay particles are closely rearranged because heating reduces the thickness of the adsorbed water layer on the surface of soil particles. As a result, the specimen develops a new structure, exhibiting higher stiffness against subsequent loading.

It may be also considered that some types of structure are created during the loading process in the CRS test and its creation is considerably accelerated under high temperature conditions. Let us reexamine the temperature and strain rate effects on the $\varepsilon^{vp} - \log p'$ relationships measured in this study in terms of structure created by heating. To compare the strain rate effect on $\varepsilon^{vp} - \log p'$ relationships, R^{vp} is defined as the ratio of p' to the corresponding value on the $ESRL_0^{vp}$ for a same ε^{vp} value (Tsutsumi and Tanaka, 2011). The stress ratio R^{vp} loops along the changes in $\dot{\varepsilon}^{vp}$ at two different temperatures are compared in Fig. 8(a) through (c), where Points b through f

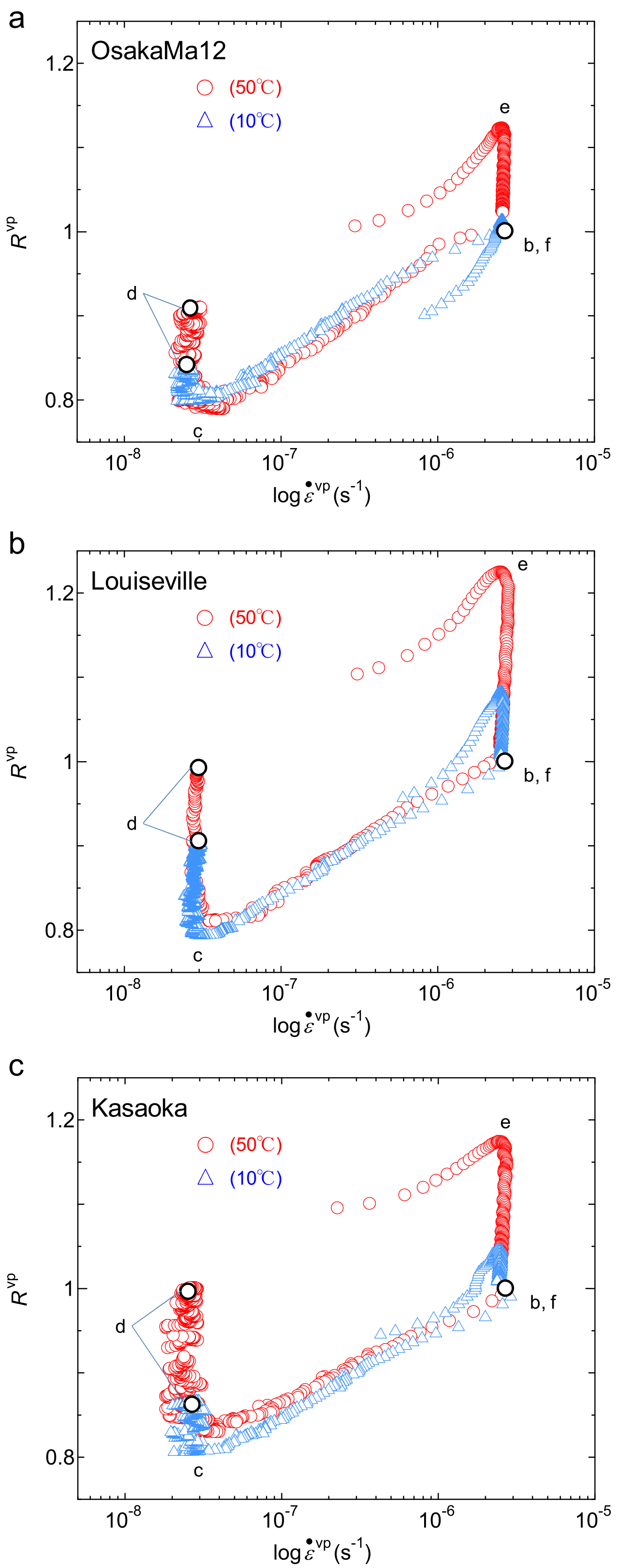

Fig. 8. Strain rate effect under different temperature for (a) OsakaMa12, (b) Louiseville and (c) Kasaoka.

correspond to those in Fig. 6(a) through (c), indicating the strain rate changes. The loop starts at Point b and its strain rate is $\dot{\varepsilon}_0^T$ so that R^{vp} is 1.0 for both temperatures. Then, $\dot{\varepsilon}^T$ is suddenly changed at Point b from reference $\dot{\varepsilon}_0^T$ to $\dot{\varepsilon}_0^T/100$, but $\dot{\varepsilon}^{vp}$ changes more gradually due to the negative $\dot{\varepsilon}^e$ generated by a decrease in p' along the transit phase of "b–c". Since $\Delta\varepsilon^{vp} - \log (p'/p'_1)$ relation shifts to the left side in this phase, R^{vp} becomes small. In this transit phase of "b-c", R^{vp} and $\dot{\varepsilon}^{vp}$ relationships are almost independent of T: i.e., the minimum value of R^{vp} at the change in the strain rate is not influenced by T. After $\dot{\varepsilon}^{vp}$ becomes constant at $\dot{\varepsilon}_0^{vp}/100$ and enter the phase "c–d", R^{vp} should not change and would indicate a single value, if the tested specimens were to exactly follow the Isotaches model. However, as already mentioned, there is a trend that $\Delta\varepsilon^{vp} - \log$ (p'/p'_1) relation is not parallel with the $ESRL_0^{vp}$, but approaches the $ESRL_0^{vp}$. Therefore, R^{vp} increases even at constant $\dot{\varepsilon}_0^{vp}/100$ especially under high temperature. When $\dot{\varepsilon}^T$ was increased along the phase of "d–e–f", the situation was opposite to that of decreasing $\dot{\varepsilon}^T$. In the transit phase of "d–e", R^{vp} increased with an increase in $\dot{\varepsilon}^{vp}$ and exceeded 1.0 when the strain rate returned to its original value. However, as the specimen is deformed further more under constant $\dot{\varepsilon}_0^{vp}$, a relatively larger rate, in the steady state of "e–f", R^{vp} gradually decreases and becomes 1.0 when the specimen returns to its original $ESRL_0^{vp}$.

It is inferred that when $\dot{\varepsilon}^{vp}$ was small, such as in the phase of "c–d", a structure was created during the loading process and the creation of the structure was accelerated by heating. Therefore, the increase in R^{vp} and the tendency of $\Delta\varepsilon^{vp} - \log$ (p'/p'_1) relation approaching the $ESRL_0^{vp}$ under high temperature conditions are prominent. Also, when $\dot{\varepsilon}^{vp}$ is returned to the original strain rate, R^{vp} exceeds 1.0 and $\Delta\varepsilon^{vp} - \log(p'/p'_1)$ relation overshoots considerably the $ESRL_0^{vp}$, like an aged clay. However, the reason for the identical R^{vp} and $\dot{\varepsilon}^{vp}$ relationships at the changing $\dot{\varepsilon}^{vp}$ such as the transit phase of "b–c" for high and low temperatures may be attributed to loading time. This duration is too short to create the structure even under high temperature. In other words, the specimen exhibits truly viscous behavior in this process.

5. Conclusions

To examine the combined effects of temperature and strain rates on the consolidation behavior of clays, a series of CRS tests, in which the strain rate was not constant but changed during consolidation, was carried out at temperatures of 10 and 50 °C for reconstituted clay samples: OsakaMa12, Louiseville and Kasaoka. The following conclusions were drawn:

1) The hydraulic conductivity of all studied clays was strongly dependent on temperature. The reason for this is that the water viscosity increases with a decrease in temperature. As a result, the excess pore water pressure generated in the specimen at 10 °C was much higher than that at 50 °C.
2) The yield effective stress decreased with increasing temperature, indicating that the clay specimens exhibited viscous behavior by heating. However, such a viscous

effect disappeared with a decrease in the void ratio (e) during a subsequent loading: under the higher level of the effective stress (p').

3) The slope of the $e-\log p'$ curve at 50 °C at the normally consolidated state, i.e., the compression index, C_c was smaller than that at 10 °C. The reason for small C_c under high temperature may be attributed to the structure created. This explanation may be applied to the observed phenomenon of overshooting the $e-\log p'$, when the strain rate was increased.
4) The structure resisting the external deformation is developed not only by high temperature but also by small strain rates. For these conditions, the Isotache model, which is simply based on viscous properties, cannot be applied to compression behavior under small strain rates, as reported by Tsutsumi and Tanaka (2011).

Acknowledgments

The authors would like to thank Drs. Y. Watabe and M. Tanaka at the Port and Airport Research Institute for providing soil samples of OsakaMa12 and Louiseville. The authors are also grateful to Mr. N. Shimakawa of Hokkaido University for conducting the CRS tests.

References

Akagi, H., 1994. A physico-chemical approach to the consolidation mechanism of soft clays. Soils and Foundations 34 (4), 43–50.

Akagi, H., Komiya, K., 1995. Constant rate of strain consolidation properties of clayey soil at high temperature. In: Proceedings of the International Symposium on Compression and Consolidation of Clayey Soils (IS-Hiroshima's 95), Hiroshima, vol. 1, pp. 3–8.

Boudali, M., Leroueil, S., Srinivasa Murthy, B.R., 1994. Viscous behaviour of natural clays. In: Proceedings of the 13th International Conference on Soil Mechanics and Foundation Engineering, New Delhi, India, vol. 1, pp. 411–416.

Campanella, R.G., Mitchell, J.K., 1968. Influence of temperature variations on soil behavior. ASCE Journal of SMFE 94 (3), 709–734.

Eriksson, L.G., 1989. Temperature effects on consolidation properties of sulphide clays. In: Proceedings of the 12th International Conference on Soil Mechanics and Foundation Engineering, Rio de Janeiro, Brazil, vol. 3, pp. 2087–2090.

Graham, J., Tanaka, N., Crilly, T., Alfaro, M., 2001. Modified Cam-Clay modeling of temperature effects in clays. Canadian Geotechnical Journal 38, 608–621.

Imai, G., Tang, Y., 1992. A constitutive equation of one-dimensional consolidation derived from inter-connected tests. Soils and Foundations 32 (2), 83–96.

Imai, G., Tanaka, Y., Saegusa, H., 2003. One-dimensional consolidation modeling based on the isotach law for normally consolidated clays. Soils and Foundations 43 (4), 173–188.

Japanese Standards Association, 2009a. Test methods for permeability of saturated soils. JIS A 1218 (2009) in Japanese.

Japanese Standards Association, 2009b. Test method for one-dimensional consolidation properties of soils using constant rate of strain loading. JIS A 1227 (2009) in Japanese.

Kobayashi, M., Furudoi, T., Suzuki, S., Watabe, Y., 2005. Modeling of consolidation characteristics of clays for settlement prediction of Kansai International Airport. In: Proceedings of the Symposium on Geotechnical Aspects of Kansai International Airport, Osaka, pp. 65–76.

Laloui, L., Leroueil, S., Chalindar, S., 2008. Modelling the combined effect of strain rate and temperature on one-dimensional compression of soils. Canadian Geotechnical Journal 45, 1765–1777.

Leroueil, S., Kabbaj, M., Tavenas, F., Bouchard, R., 1985. Stress–strain-strain rate relation for the compressibility of sensitive natural clays. Geotechnique 35 (2), 159–180.

Leroueil, S., 2006. Suklje's memorial lecture—the isotache approach: where are we fifty years after its development by Professor Suklje?. In: Proceedings of the European-Danube Conference on Geotechnical Engineering, Ljubljana, vol. 1, pp. 55–88.

Marques, M.E.S., Almeida, M.S.S., Leroueil, S., 2004. Viscous behaviour of St-Roch-de-l'Achigan clay, Quebec. Canadian Geotechnical Journal 41, 25–38.

Moritz, L., 1995. Geotechnical properties of clay at elevated temperatures. In: Proceedings of the International Symposium on Compression and Consolidation of Clayey Soils (IS-Hiroshima's 95), Hiroshima, vol. 1, pp. 267–272.

Moriwaki, T., Umehara, K., 2003. Method for determining the coefficient of permeability of clays. Geotechnical Testing Journal 26 (1), 47–56.

National Institutes of Natural Sciences, National Astronomical Observatory of Japan, 2004. Chronological Scientific Tables in Japanese.

Šuklje, L., 1957. The analysis of the consolidation process by the isotache method. In: Proceedings of the 4th International Conference on Soil Mechanical Found. Engineering, London, vol. 1, pp. 200–206.

Tanaka, H., 2005a. Consolidation behavior of natural soils around p_c value—long term consolidation test. Soils and Foundations 45 (3), 83–96.

Tanaka, H., 2005b. Consolidation behavior of natural soils around p_c value—inter-connected oedometer test. Soils and Foundations 45 (3), 97–105.

Tatsuoka, F., Di Benedetto, W., Enomoto, T., Kawabe, S., Kongkitkul, W., 2008. Various viscosity types of geomaterials in shear and their mathematical expression. Soils and Foundations 48 (1), 41–60.

Towhata, I., Kuntiwattanaku, P., Seko, I., Ohishi, K., 1993. Volume change of clays induced by heating as observed in consolidation tests. Soils and Foundations 33 (4), 170–183.

Tsuchida, T., Kobayashi, M., Mizukami, J., 1991. Effect of ageing of marine clay and its duplication by high temperature consolidation. Soils and Foundations 31 (4), 133–147.

Tsutsumi, A., Tanaka, H., 2011. Compressive behavior during the transition of strain rate. Soils and Foundations 51 (5), 813–822.

Tsutsumi, A., Tanaka, H., Kawaguchi, T., 2011. Validity of Isotache model for Osaka and Louiseville intact clays. In: Proceedings **of** the 14th Asian Regional Conference on Soil Mechanics and Geotechnical Engineering, 14th ARC 2011, Hong Kong, China, (on CD-ROM).

Watabe, Y., Udaka, K., Morikawa, Y., 2008. Strain rate effect on long-term consolidation of Osaka bay clay. Soils and Foundations 48 (4), 495–509.

Yashima, A., Leroueil, S., Oka, F., Guntoro, I., 1998. Modelling temperature and strain rate dependent behavior of clays: one dimensional consolidation. Soils and Foundations 38 (2), 63–73.